Dyes and Pigments 80 (2009) 264–270

Contents lists available at ScienceDirect

Dyes and Pigments

journal homepage: www.elsevier.com/locate/dyepig

The influence of synthesis conditions on the crystal and aggregate properties of calcium salt azo pigment CI Pigment Red 48:2

R.M. Christie*, I. Chugtai, R.R. Mather

School of Textiles and Design, Heriot-Watt University, Scottish Borders Campus, Galashiels TD1 3HF, Scotland, UK

ARTICLE INFO

Article history:
Received 20 June 2008
Accepted 18 July 2008
Available online 29 July 2008

Keywords:
Calcium salt azo pigment
Nitrogen adsorption
Transmission electron microscopy
Aggregate

ABSTRACT

The influence of pH and heating time at 80 °C on the final stage (conversion to the calcium salt) of the formation of the metal salt azo pigment, CI Pigment Red 48:2, has been investigated. A series of systematically prepared pigment samples were characterized by transmission electron microscopy, X-ray powder diffraction, surface area measurement and a detailed nitrogen adsorption–desorption isotherm investigation. Significant differences in the crystal sizes and morphologies and in the crystal growth patterns were observed. The colour and lightfastness properties in air-drying alkyd paints are correlated with the physical property data.

1. Introduction

The most important red classical organic pigments are azo pigments obtained from 2-naphthol and its derivatives as coupling components [1–4]. In this group, metal salt azo pigments derived from 3-hydroxy-2-naphthoic acid (βONA) are of greatest commercial significance. The metal ions most commonly used are derived from the alkaline earths and the transition metal, manganese. The pigments are products of high colour strength and brightness, high transparency and good solvent resistance, properties which are particularly suited to printing ink applications, although they are also used to a certain extent in the coloration of coatings and thermoplastics. CI Pigment Red 48:2 (**1**), commonly referred to as Ca2B toner, is a product of particular industrial importance. It is now clearly established that pigments of this type exist as the ketohydrazone rather than as the azo form [1]. No X-ray crystal structural determination of **1** has been reported, but that of a very closely related pigment sheds considerable light on the complex supramolecular structure of these pigments in the solid state [5]. The calcium atoms are eight-coordinate through bonding to three oxygens (carboxylate, keto and sulphonate) in one ligand anion, to two terminal water molecules and to three oxygen atoms supplied by bridging to the carboxylate groups of neighbouring anions. The bridging leads to a polymeric ladder structure, with a double chain of calcium atoms and with coordinated water ligands either side of the ladder.

The preparation of **1**, as illustrated in Scheme 1, involves azo coupling of diazotized 2-chloro-4-toluidine-5-sulphonic acid (2B acid) (**2**) with 3-hydroxy-2-naphthoic acid (**3**) under alkaline conditions to give the disodium salt (**4**) which is subsequently converted to the calcium salt by treatment with calcium chloride [4,6]. It is well-known within the industry that the conditions of synthesis and subsequent conditioning of azo pigments have an important influence on their crystalline solid state properties, including particle size and shape distribution and the aggregate structure, which in turn significantly affect the application performance of the pigments. However, there have been relatively few reported detailed quantitative studies of these effects for specific pigments, especially of the metal salt azo type. This paper describes a study of the effect of pH and heat treatment time, two important manufacturing variables, during the conversion to the calcium salt on the particle and aggregate structure of CI Pigment Red 48:2, characterized using a combination of nitrogen adsorption, X-ray powder diffraction and transmission electron microscopic techniques. The solid state properties are correlated with the colouristic and technical performance of the pigments incorporated into air-drying paints.

2. Experimental

2.1. Instrumental methods

2.1.1. Nitrogen gas adsorption

Nitrogen adsorption isotherms were determined at 77 K by a volumetric method, with a semi-micro apparatus of the type designed by Harris and Sing [7]. The nitrogen, of >99% purity, was

* Corresponding author.
E-mail address: r.m.christie@hw.ac.uk (R.M. Christie).

0143-7208/$ – see front matter © 2008 Elsevier Ltd. All rights reserved.
doi:10.1016/j.dyepig.2008.07.011

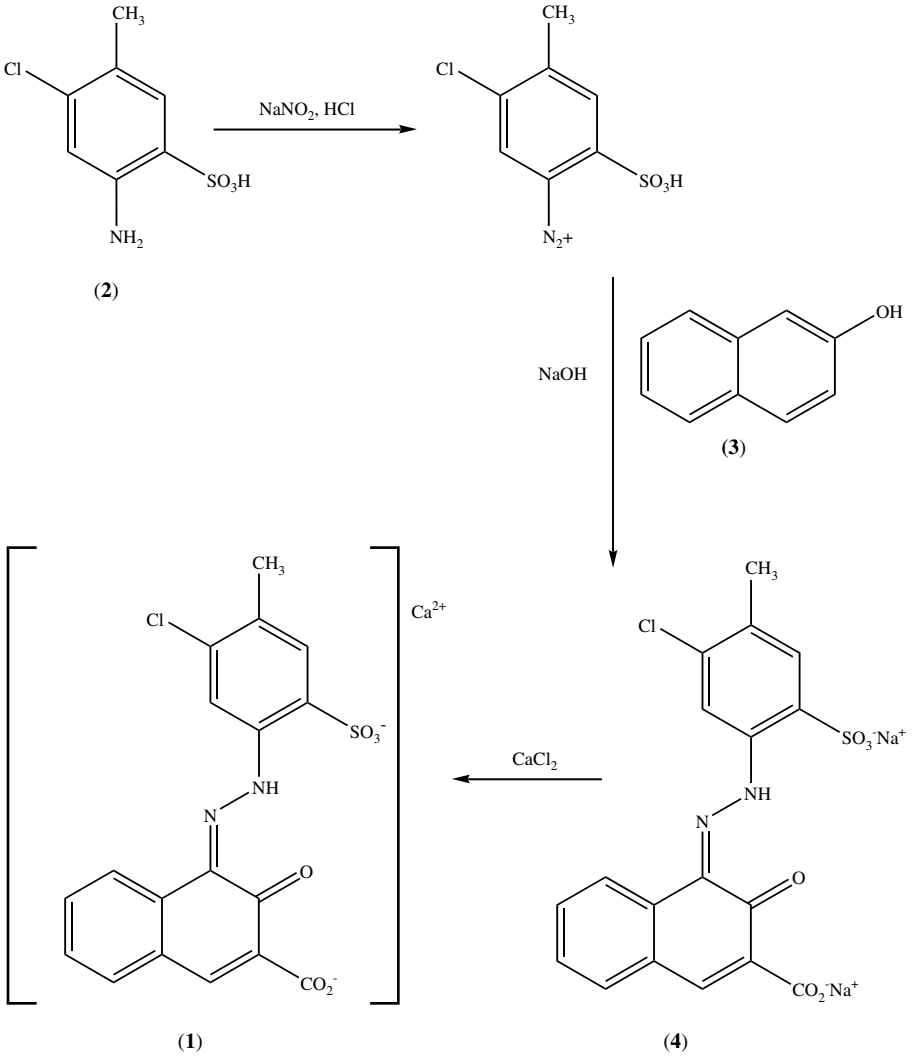

Scheme 1. Synthesis of CI Pigment Red 48:2.

dried by slow passage through a liquid nitrogen trap. Before the start of an isotherm determination, each pigment sample was evacuated for at least 18 h at room temperature. Equilibrium pressures were measured with the aid of a cathetometer (to ±0.002 cm).

2.1.2. X-ray powder diffraction

X-ray powder diffraction traces were obtained using a Siemens D-500 diffractometer. The pigment samples were ground to a fine powder, inserted into the metal plate with an aperture of 0.8 mm and the trace recorded with a monochromated X-ray beam of Cu Kα radiation ($\lambda = 1.54$ Å), using a scan speed of 0.02 degrees s^{-1}. From the peak of greatest intensity in the diffraction traces, at $2\theta \sim 4.5°$, mean crystallite thicknesses, Z_c, were calculated using the Debye–Scherrer (Eq. (1)).

$$Z_c = K\lambda/\beta_{1/2} \cos\theta \quad (1)$$

where K (shape constant) = 0.9 and $\beta_{1/2}$ is the mean of the width of the peaks measured at half their height. A similar approach has been adopted using the X-ray diffraction patterns of samples of the structurally related pigment, CI Pigment Red 57:1 [8].

2.1.3. Transmission electron microscopy

The micrographs were obtained on a Philips EM 300 Transmission Electron Microscope with an exposure time of 4 s at a total magnification of 60,000 or less depending on the size of the crystals. For sample preparation, the pigments were dispersed ultrasonically in ethanol, one drop placed on the carbon grid and the solvent allowed to evaporate. The micrographs were supplied by Dr. R.B. McKay, Ciba Specialty Chemicals, Hawkhead Rd., Paisley, Scotland. Several micrographs were examined for each sample.

*2.2. Synthesis of CI Pigment Red 48:2 (**1**)*

2-Chloro-4-toluidine-5-sulphonic acid (2B acid) (**2**) (221.5 g, 1.0 mol) was dissolved in a solution of sodium hydroxide (64 g) in water (5 l). Ice was added to bring the temperature below 5 °C, followed by the addition of concentrated hydrochloric acid (400 cm^3). A solution of sodium nitrite (72 g, 1.04 mol) in water (1 l) was added and the suspension stirred for 15 min while maintaining the temperature below 5 °C by the addition of ice, when necessary. The presence of a nitrous acid excess of sodium nitrite was indicated using starch/KI paper. The suspension was stirred for a further 30 min. Just before the coupling, a few drops of aqueous sulphamic acid solution were added to destroy excess nitrous acid. The diazonium salt suspension was added slowly to a solution of 2-hydroxy-3-naphthoic acid (188 g, 1.0 mol) (**3**) and sodium hydroxide (201 g) in water (5500 cm^3). The pH level was monitored during the reaction and adjusted using a 2 M solution of sodium hydroxide, if it fell below 12. The reaction was checked frequently

to ensure an absence of excess diazonium salt, using the H-acid spot test. After coupling the suspension of the disodium salt of the azo dye was divided into six equal portions. The pH of the portions of the suspension was adjusted using dilute hydrochloric acid to the values shown in Table 1. A solution of calcium chloride (37.5 g, 0.4 mol) in water (200 cm^3) was added to each portion and the mixture was stirred for 15 min at ambient temperature. The suspension was then heated at 80 °C for heating times as indicated in Table 1. The suspension was then filtered hot and washed with water in order to remove inorganic salts, and finally the samples were dried using a freeze drier, to minimise hydrophilic aggregation.

2.3. Application properties

2.3.1. Preparation of alkyd resin based air-drying gloss paint

The pigment was passed through a 100-μm sieve before incorporation into the paint. Pigment (3 g) was inserted into a honey jar together with Uralac P470, a long oil alkyd resin (3 g) and white spirit (24 g). The mixture was mixed well with a spatula until the pigment was thoroughly wetted with the resin and solvent. Ceramic balls (100 g) were added into the honey jar, which was then closed and sealed with polythene tape. The jar was rotated on ball mill rollers at 120 rpm for 16 h. Uralac P470 resin (40 g) and driers (a solution of cobalt and zirconium octanoates in white spirit, 2 g) were then added. The paint preparation was completed after a further 30 min of milling. The paint was discharged into a paper cup and allowed to stand for at least 1 h to de-aerate before use. For white reductions, the coloured paints were mixed with ICI Dulux Brilliant White gloss paint at a ratio of 1:2. Drawdowns on Astralux card were prepared from these paints using a 100-μm bar. The films were left to air dry for 2–3 days.

2.3.2. Colour measurement

Colour measurement was carried out using a Datacolor Spectraflash SF600 reflectance spectrophotometer which was calibrated using the black and white reference tiles supplied by the manufacturer. The instrument was set to measure using the large aperture, with specular reflectance excluded and UV included. Colour difference values were computed using illuminant D65 and 10° observer data.

2.3.3. Lightfastness

The dried paint films were tested on a Heraeus Xenotest 150S instrument. The samples were exposed constantly with one side covered for 300 h under the Xenon arc light. The photofading of the samples was assessed as the colour difference between exposed and unexposed areas of the paint films.

3. Results and discussion

CI Pigment Red 48:2 (**1**) was prepared as illustrated in Scheme 1. The final stage in the process during which the pigment forms involves calcium salt formation. This conversion was carried out at a temperature of 80 °C, typical of commercial processes, but using different pH conditions (weakly acidic, neutral and alkaline) and heating times (15 min and 1 h) as described in Table 1. For the purpose of this investigation on the pigment in isolation, additives such as surfactants, resins and other auxiliaries were specifically excluded, although these materials are commonly incorporated in optimised commercial products.

Table 1
Mean crystallite thickness (Z_c) and surface area of samples of CI Pigment Red 48:2 (**1**) prepared using different pH values and heat treatment times

Sample	pH	Heating time (80 °C)	Mean crystallite thickness, Z_c (nm)	Nitrogen isotherm data		
				S_{BET} ($m^2\,g^{-1}$)	c	r
1a	5.0	15 min	17.9	68.1	64	2.04
1b	5.0	1 h	20.8	62.2	35	2.01
1c	7.0	15 min	27.8	32.8	78	2.02
1d	7.0	1 h	27.8	19.9	52	1.78
1e	11.0	15 min	22.6	82.1	53	1.93
1f	11.0	1 h	32.1	31.9	62	1.92

Selected representative transmission electron micrographs of the pigment samples are shown in Fig. 1a–f. The micrographs demonstrate that both the pH used for the conversion and the heat treatment time have a significant influence on the size and morphology of the pigment crystals formed. Inspection of the micrographs reveals that the crystals of all six pigment samples are plate-like and this allows an estimation of the two large dimensions. In many of the micrographs studied, a few thin crystal faces could also be observed, as highlighted in Fig. 1e for example, allowing some estimation of the much smaller third dimension. The plate-like nature of the crystals resembles that of crystals of CI Pigment Red 57:1, commonly referred to as Ca4B toner, a rubine pigment of wide commercial application whose chemical constitution is very similar to CI Pigment Red 48:2 (**1**) differing only in that the chlorine substituent is absent [8].

The crystals of sample **1a**, resulting from a heat treatment of 15 min at pH 5, are mostly quite squat, with a thickness of ca. 18 nm. The two larger dimensions vary considerably between 0.05 μm and 0.12 μm, although a number of crystals appear broader still. Heat treatment for 1 h at pH 5 (**1b**) produces bigger, better developed crystals, with lengths and breadths of up to 0.14 μm or even greater, and a thickness generally of 18–20 nm. In contrast, heat treatments at pH 7 produce much larger and broader pigment crystals than those produced at pH 5. In addition, the crystals possess more rectangular shapes. After 15 min of heat treatment (**1c**), the breadth of the crystals is mostly 0.15–0.20 μm, and the length up to 0.8 μm. The thickness of the crystals appears to be 15–20 nm. Heat treatment for 1 h (**1d**) produces crystals of breadth ca. 0.4 μm, maximum length in excess of 2 μm and thickness ca. 50 nm. Heat treatment for 15 min at pH 11 (**1e**) gives rise to small crystals of a similar appearance to those produced over the same time period at pH 5. It is noteworthy that for pigment **1e**, the thickness of up to as many as 14 crystals could be assessed: 15–20 nm. After 1 h treatment at pH 11, there is clearly extensive growth (**1f**). Well-defined crystals are produced, generally of width ca. 0.14–0.20 μm and length up to ca. 0.5 μm, although a few crystals are larger still. Of the very few crystals whose thin crystal faces were observed for this sample, values for crystal thickness of 20–30 nm were obtained.

The locations of the peaks in the X-ray powder diffraction traces for all six pigment samples are virtually identical, so that no differences in crystal lattice structure are revealed. The traces for samples **1a** and **1b** are given in Fig. 2 as examples. However, longer heat treatments at all three pH values give rise to sharper peaks in the diffraction traces, indicating enhanced crystallinity. The mean crystallite thicknesses, Z_c, estimated from the diffraction peaks at $2\theta \sim 4.5°$, are given in Table 1 [8]. For samples **1a** and **1b**, heat treated at pH 5.0, the crystallite thicknesses are similar to those assessed from transmission electron micrographs. For samples **1e** and **1f**, heat treated at pH 11.0, the thicknesses estimated from the X-ray traces appear slightly greater than those assessed from transmission electron micrographs. Discrepancies are, however, apparent for samples **1c** and **1d**. The crystallite thickness estimated for **1c** is greater than that assessed from the micrographs while for **1d**, the crystallite size assessed from the micrographs is the larger value. It is interesting to note that identical values for **1c** and **1d** are estimated from the X-ray traces.

Fig. 3a–f shows the nitrogen adsorption–desorption isotherms determined on the six pigment samples. Analysis and interpretation

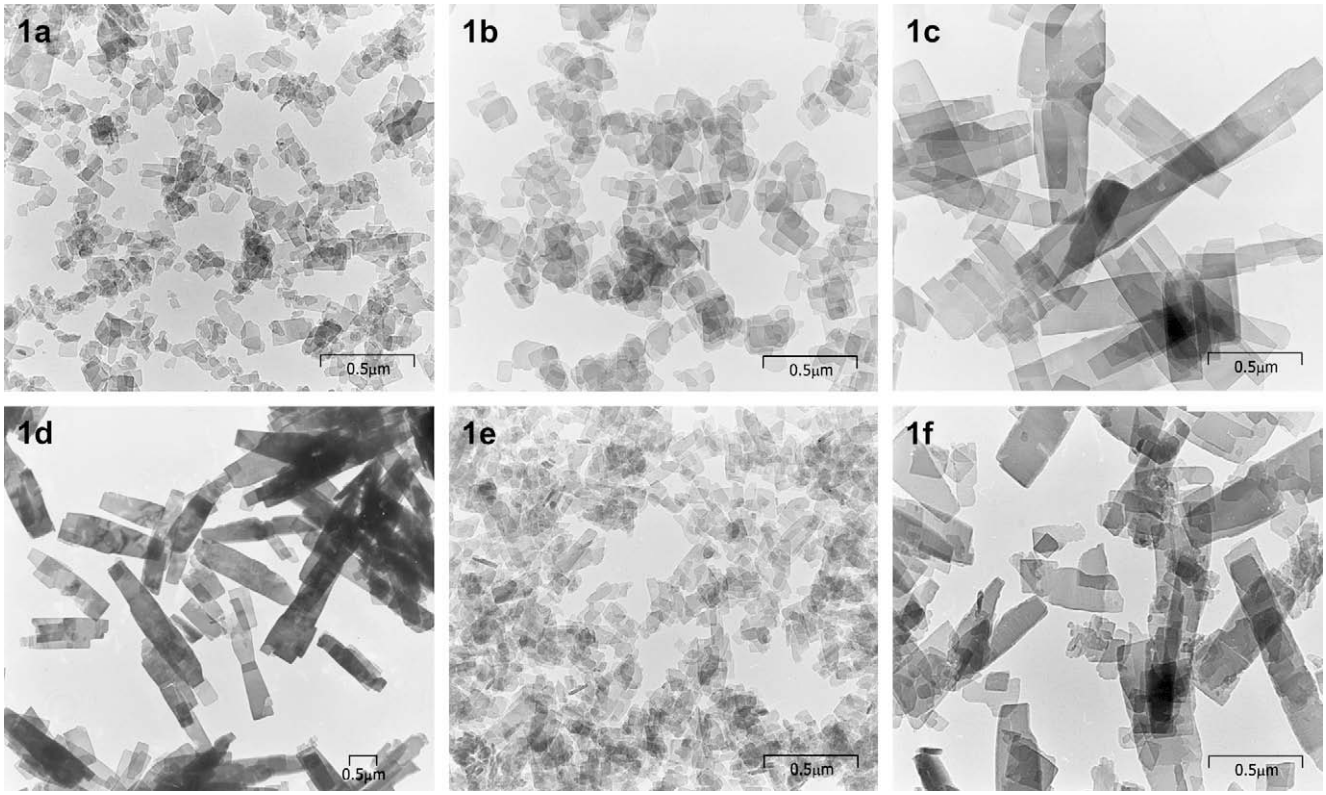

Fig. 1. Transmission electron micrographs of samples **1a**–**1f** of Ca2B toner.

of nitrogen isotherms from organic pigment samples have been extensively discussed elsewhere [9–11]. Table 1 lists the specific surface areas, S_{BET}, determined from application of the Brunauer–Emmet–Teller (BET) equation [12] to the low pressure region of the isotherm (relative pressures < 0.4). Values for the BET parameter, *c*, were also determined. The *c*-values provide broad comparisons of the strength of interaction between the pigment crystal surface and adsorbed nitrogen molecules. Where the pigment samples are all of the same chemical composition, as in the present case, significant differences in *c*-values can generally be attributed to differences in microporosity (pores < 2 nm in width [13]) amongst the samples, lower *c*-values indicating less microporosity.

Also listed in Table 1 are values of the Frenkel–Halsey–Hill (FHH) parameter, *r*, determined from the FHH equation at relative pressures from 0.4 upwards [13]. Differences in the value of *r* amongst the samples indicate differences in mesoporosity (pores of 2–50 nm in width [13]). Values in the range 2.6–2.7 in samples containing no micropores are consistent with the absence also of mesopores. The lower the *r*-value, the more mesoporous is the sample. The presence of micropores in a sample tends to raise the value of *r* [14].

The adsorption branches of all the isotherms in Fig. 3 exhibit a sigmoidal shape. In many of the isotherms, the paths of the desorption branches virtually coincide with those of the adsorption branches, although in Fig. 3a and e, the desorption branches lie slightly above the adsorption branches. These isotherm characteristics have been observed previously in a variety of organic pigments [8,9].

The nitrogen isotherms for samples **1a** and **1b**, heat treated at pH 5, are shown in Fig. 3a and b, respectively. The isotherm for **1a** (heat treatment for 15 min) exhibits an adsorption–desorption hysteresis loop at relative pressures above ca. 0.4. Such hysteresis is associated with the presence of mesopores between adjacent crystals caused by the aggregation of pigment crystals [9]. In contrast, the isotherm shown in Fig. 3b (1 h heat treatment) appears reversible in that it exhibits no clear hysteresis. Table 1 reveals that prolonging the heat treatment at pH 5 slightly lowers specific surface area, a result consistent with the slight increase in pigment crystal size observed by transmission electron microscopy. There is also a large decrease in *c*-value from 64 to 35, which can be ascribed to a considerable reduction in microporosity. In organic pigment samples, the presence of micropores arises from very narrow spaces of <2 nm between adjacent pigment crystals. Values of *c* in the range 30–40 have been found in samples of copper phthalocyanine pigments [9]. In these samples, microporosity appears to be absent, and so we suggest that the 1 h heat treatment virtually eliminates microporosity.

The removal of hysteresis from the isotherm as a result of longer heat treatment at pH 5 at first sight would appear to reveal reduced

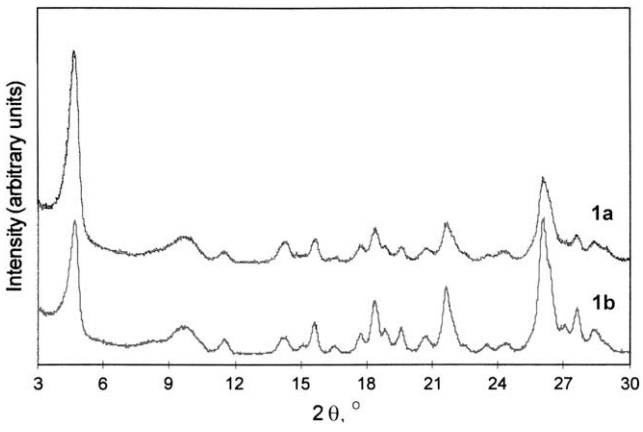

Fig. 2. X-ray powder diffraction traces for samples **1a** and **1b**.

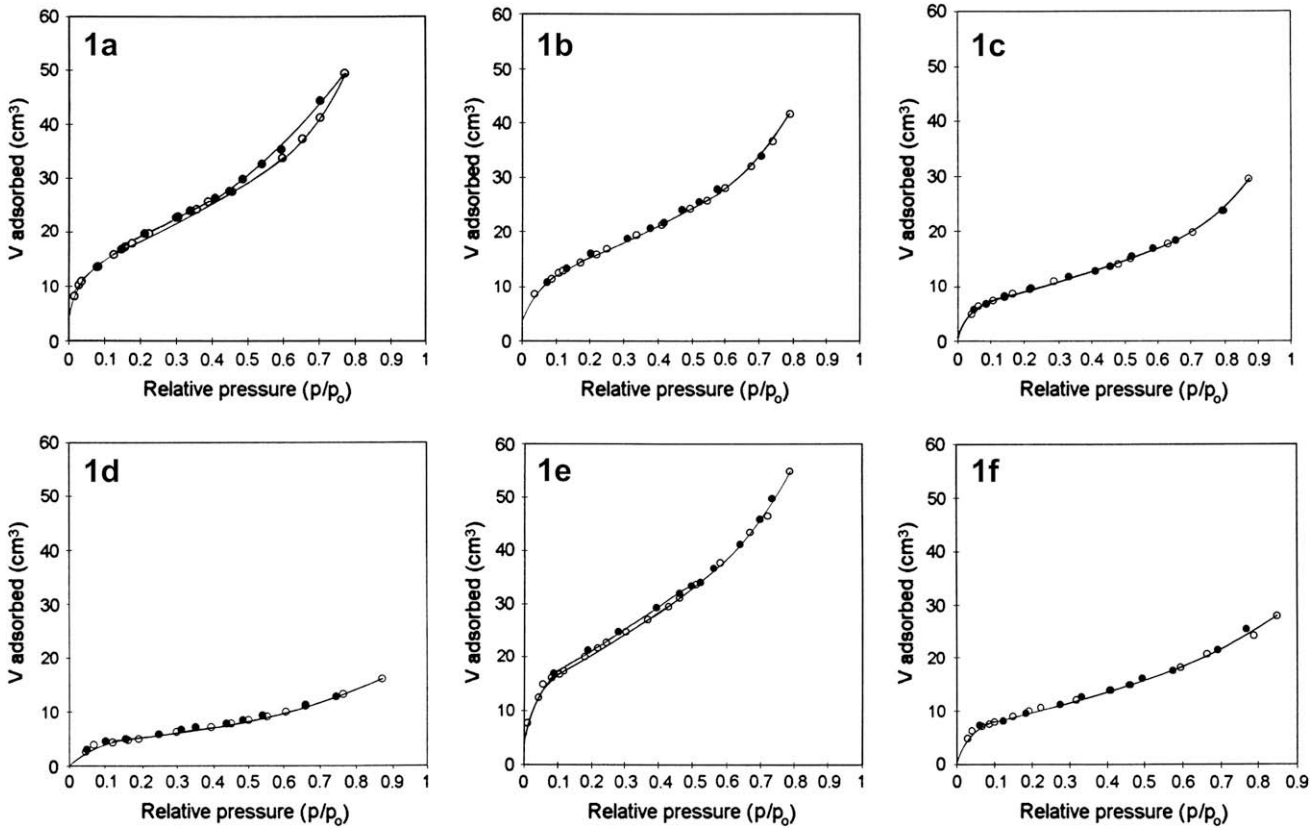

Fig. 3. Nitrogen adsorption–desorption isotherms for samples **1a**–**1f**.

aggregation. Similar changes in isotherm behaviour have been noted with copper phthalocyanine pigment samples [15]. However, these changes were accompanied by much larger increases in crystal size than observed here. Moreover, the *r*-value for pigment **1b** is only 2.01, much lower than that expected if no mesopores are present. This observation can be reconciled with the absence of hysteresis at higher relative pressures in Fig. 3b, if the mesopores are now predominantly wedge-shaped or conical. Such mesopores do not give rise to hysteresis in an isotherm [16]. The *r*-value, 2.04, for pigment **1a** is also consistent with the extensive mesoporosity revealed by the hysteresis loop in Fig. 3a. Indeed, the value is likely to be slightly elevated due to the presence of micropores in the sample.

The isotherms for samples **1c** and **1d**, heat treated at pH 7, are shown in Fig. 3c and d, respectively. Both isotherms appear reversible. The values of S_{BET} for these two pigments are considerably lower than for samples **1a** and **1b**, a feature consistent with their larger crystal sizes. Table 1 also shows that prolonging the heat treatment from 15 min to 1 h lowers S_{BET} by ca. 40%, and indeed transmission electron microscopy (Fig. 1) reveals that the blade-like crystals of sample **1d** are, on average, much larger than those of sample **1c**. As at pH 5, prolonging the heat treatment at pH 7 also considerably reduces the *c*-value, although the value of 52 for sample **1d** suggests that, whilst the extent of microporosity is lowered, it has not been eliminated. The FHH *r*-values of the two samples are both low, especially that of sample **1d**. As with sample **1b**, extensive wedge-shaped mesoporosity is indicated in both samples, even though their isotherms appear virtually reversible.

The isotherms for samples **1e** and **1f**, heat treated at pH 11, are shown in Fig. 3e and f, respectively. The isotherm for sample **1e** appears to show a small, but significant level of hysteresis, even down to low relative pressures. Where low pressure hysteresis occurs in the isotherms of pigment samples, it is attributed to the presence of crystal aggregates that possess quite loose structures [9]. Little or no hysteresis is apparent for sample **1f**. Table 1 shows that a more prolonged heat treatment massively reduces S_{BET}, and indeed transmission electron microscopy has shown a huge increase in the size of the pigment crystals. The increase in the BET *c*-value is small, but probably significant, and suggests some increase in microporosity. The FHH *r*-values are virtually identical, though the *r*-value for sample **1f** would be somewhat higher than for sample **1e**, if microporosity were absent. Both *r*-values are, however, low, and again may arise from the presence of wedge-shaped mesopores.

An air-drying gloss paint was selected as an appropriate medium to assess technical performance based on the judgment that the aliphatic hydrocarbon solvent used in its formulation and the ambient temperature of application would be likely to have minimal influence on the crystal properties of the pigment. The colouristic properties of the samples of CI Pigment Red 48:2 are shown in Tables 2 and 3. Table 2 lists colouristic differences in full

Table 2
Colour differences in full strength air-drying gloss paints from samples of CI Pigment Red 48:2, relative to standard sample **1b**

Sample	Colour difference, ΔE	Lightness difference, ΔL^*	Chroma difference, ΔC^*	Hue difference,[a] ΔH^*
1a	0.32	−0.12	−0.30	0.01
1b	0.00	0.00	0.00	0.00
1c	2.25	0.06	−2.20	0.43
1d	4.11	−0.45	−4.08	0.22
1e	0.29	−0.25	−0.01	−0.15
1f	3.34	−0.52	−3.30	0.20

[a] Positive values are yellower than standard, negative values bluer.

Table 3
Colour differences in white reduced paint from samples of CI Pigment Red 48:2, relative to standard sample **1b**

Sample	Colour difference, ΔE	Lightness difference, ΔL^*	Chroma difference, ΔC^*	Hue difference,[a] ΔH^*
1a	0.74	0.58	0.44	0.13
1b	0.00	0.00	0.00	0.00
1c	7.02	3.25	−6.19	0.68
1d	10.77	4.65	−9.64	1.22
1e	3.26	0.12	3.19	0.69
1f	6.78	2.72	−6.21	0.13

[a] Positive values are yellower than standard, negative values bluer.

strength gloss paints while Table 3 shows the differences in white reductions prepared from the full strength paints. In all cases, the differences are calculated against the data of sample **1b** selected as the standard for comparison, on the basis that this pigment sample appears to consist of crystals that are essentially free of aggregation. From the tables, it can be deduced that prolonging heat treatment from 15 min to 1 h results in reduction in chroma, largely indicative of a reduction in colour strength, in the samples treated at pH 7 and pH 11, although not in the sample prepared at pH 5. This is due to the significant crystal growth with time at the higher pH values which is illustrated by the TEMs and confirmed by the lower surface area values. At pH 5, there is less pronounced crystal growth with time and it is accompanied by improved crystallinity and by apparent deaggregation, which probably leads to improved dispersion in the application, so that there is little overall effect on the colouristics. There are no particularly significant differences in lightness and hue in full strength paints. The effect of longer heat treatment is more apparent in the colour properties of the white reductions than in the full strength paints. For heat treatments at pH values 7 and 11, the colour differences are again associated with a pronounced decrease in chroma as heating is prolonged, although in these cases there is also an increase in lightness and a marginal hue shift. Again the samples prepared at pH 5 show little change in colour properties with the longer heating time, attributed to the competing effects of crystal growth and deaggregation. The differences in chroma are broadly in line with expectations from the differences in crystal sizes/surface area, with sample **1e** ($S_{BET} = 82.1\ m^2\ g^{-1}$) showing highest chroma and sample **1d** ($S_{BET} = 19.9\ m^2\ g^{-1}$) showing lowest chroma (and highest lightness).

Lightfastness results for 300 h. Xenotest exposure are given in Table 4. These are expressed as a colour difference between exposed and unexposed areas of the paint films so that a lower value indicates improved lightfastness. In general, it is to be expected that lightfastness would improve with an increase in particle size (reduction in surface area) and an increase in crystallinity and that any differences would be more pronounced in white reductions. On the basis of the data on the physical properties of these pigments therefore, an improvement in lightfastness with heating time would be expected. Indeed, sample **1e** which has the most poorly defined and smallest crystals has the lowest lightfastness in both full strength and reduction. In both application media, a longer heating time at pH 11 leads to a particularly pronounced improvement in lightfastness, due to the significant enhancement of crystallinity and crystal growth observed. A similar effect is also observed in white reduction for samples prepared at pH 5. However, in full strength paints from pigments prepared at pH 5 and in both paints from pigments prepared at pH 7, lightfastness either remains essentially unchanged or deteriorates marginally. The results are thus mostly consistent with expectations, though not entirely, perhaps unsurprisingly since the lightfastness of pigments in application is a complex phenomenon dependent on many internal and external factors.

Table 4
Lightfastness of the paint films derived from samples of CI Pigment Red 48:2 after 300 h exposure, expressed as colour difference (ΔE) between exposed and unexposed areas

Sample	ΔE (full strength paint)	ΔE (white reduction)
1a	3.65	4.73
1b	4.54	2.68
1c	2.64	3.29
1d	3.34	3.33
1e	5.09	6.86
1f	3.09	2.80

4. Conclusions

In the final stage of the preparation of CI Pigment Red 48:2 (1), which involves the conversion to the calcium salt, the pH and heating time at 80 °C have a significant influence on the physical properties of the resulting pigment crystals. The pigment samples invariably show plate-like geometry with a very small third dimension. At weakly acidic pH, fairly small squat crystals form which, with prolonged heating, show some limited crystal growth (from TEM visualization and S_{BET} values from nitrogen adsorption measurements) and improved crystallinity (from XRD powder diffraction), together with some deaggregation and reduction in microporosity (from the disappearance of hysteresis in the nitrogen adsorption–desorption isotherms). At neutral pH, much larger, more rectangular, crystals form initially and these continue to grow and refine with heating. At alkaline pH, very small crystals form initially and these experience significant growth with heating. The differences in size, morphology and aggregation of the pigments are likely to be associated with the fact that in the range of pH values studied, the sulphonate group is ionized throughout, while the carboxylate group is increasingly in its protonated form as the pH is reduced. The monosodium and disodium salts of the azo dye initially formed together with the intermediate species involved in the conversion to the Ca^{2+} salt, are likely to have significantly different solubility characteristics, leading to complex crystal nucleation and growth mechanisms. The colour and lightfastness properties in an air-drying paint formulation are generally consistent with the observed differences in physical properties of the pigment samples. For application performance, heat treatment at pH 5 for 1 h would appear to offer significant advantages, as these conditions produce a highly deaggregated pigment, essentially free of microporosity, with limited crystal growth, giving small well-defined, fairly regularly shaped crystals, resulting in a product with high colour strength and reasonable lightfastness properties. At higher pH values, the pigment undergoes much more significant crystal growth to a 'blade-like' morphology.

Acknowledgements

We acknowledge the support of Ciba Specialty Chemicals, Paisley, Scotland and, in particular, Dr. R.B. MacKay for helpful discussion.

References

[1] Christie RM. The organic and inorganic chemistry of pigments. London: Oil and Colour Chemists Association; 2001.
[2] Herbst W, Hunger K. Industrial organic pigments, production, properties, applications. 1st ed. Weinheim: VCH; 1993 [2nd ed., 1997, 3rd ed., 2004].
[3] Patton TC, editor. Pigment handbook. 1st ed., vol. I. New York: John Wiley & Sons; 1973;
Lewis PA, editor. Pigment handbook. 2nd ed. New York: John Wiley & Sons; 1988.
[4] Christie RM, Mackay JL. Metal salt azo pigments. Color Technol 2008; 124:133–44.
[5] Kennedy AR, McNair C, Smith WE, Chisholm G, Teat SJ. The first red azo pigment whose structure is characterised by single crystal diffraction. Angew Chem Int Ed 2000;39:638–40.

[6] Christie RM, Moss S. Metal salt pigments derived from 3-hydroxy-2-naphthohydroxamic acid. Dyes Pigments 1987;8:211–24.
[7] Harris MR, Sing KSW. The surface properties of precipitated alumina, 1. Preparation of active-samples and determination of nitrogen adsorption isotherms. J Appl Chem 1955;5:223–7.
[8] McKay RB. Physical character of calcium 4B toner pigments and their performance in viscous printing inks. FATIPEC Congr XVIII 1986;2/B:405–25.
[9] Mather RR, Sing KSW. Surface properties of organic pigments, 1. Adsorption of argon and nitrogen on copper phthalocyanines. J Colloid Interface Sci 1977;60:60–6.
[10] Mather RR. Hysteresis in nitrogen adsorption isotherms on copper phthalocyanine pigments. Colloids Surf 1991;58:401–7.
[11] Mather RR. Evaluation by nitrogen adsorption of crystal aggregation in organic pigments. Dyes Pigments 2000;47:17–21.
[12] Brunauer S, Emmett PH, Teller E. Adsorption of gases in multimolecular layers. J Am Chem Soc 1938;60:309–19.
[13] IUPAC manual of symbols and terminology for physicochemical quantities and units – appendix 2. Colloid and surface chemistry. Pure Appl Chem 1972;31:538–77.
[14] Carrott PJM, McLeod AI, Sing KSW. Application of the Frenkel–Halsey–Hill equation to multilayer isotherms of nitrogen on oxides at 77 K. In: Rouquerol J, Sing KSW, editors. Adsorption at the gas–solid and liquid–solid interface. Amsterdam: Elsevier; 1982. p. 403–10.
[15] Fryer JR, McKay RB, Mather RR, Sing KSW. The technological importance of the crystallographic and surface properties of copper phthalocyanine pigments. J Chem Technol Biotechnol 1981;5:371–87.
[16] Gregg SJ, Sing KSW. Adsorption, surface area and porosity. 2nd ed. London: Academic Press; 1982.